Construction of WO3 quantum dots / TiO2 nanowire arrays type II heterojunction via electrostatic self-assembly for efficient solar-driven photoelectrochemical water splitting

Ning Zhang [abd#], Huili Li [c#], Bo Yao [a], Shiyan Liu [a], Jun Ren [a], Yawei Wang [e], Zebo Fang [a*], Rong Wu [bd*], Shunhang Wei [a*]

[a] Zhejiang Engineering Research Center of MEMS, Shaoxing University, Shaoxing 312000, China.

[b] School of Physics Science and Technology, Xinjiang University, Urumqi, Xinjiang 830000, China.

[c] College of Chemistry and Materials Science, Shanghai Normal University, Shanghai 200234, China.

d Xinjiang Key Laboratory of Solid State Physics and Devices, Xinjiang University, Urumqi, Xinjiang 830017, China

[e] School of Chemistry and Chemical Engineering, Jiujiang University, Jiujiang 332005, China

E-mail: csfzb@usx.edu.cn; wurongxju@sina.com; wshusx@163.com

[#] Equal contributions.

Characterization

The crystalline phases of the prepared samples were examined by a DX-2700BH X-ray powder diffractometer (XRD). The morphology was recorded by a field emission scanning electron microscope (FESEM, SIGMA 300) and a high-resolution transmission electron microscope (HRTEM, JEM-2100F) equipped with an energy dispersive X-ray spectrometer (EDS). The elemental chemical states of the samples were examined using an X-ray photoelectron spectroscopy (XPS, Thermo Scientific K-Alpha) with a monochromatic Al Kα source (1486.6 eV). All the binding energies were calibrated using the C1s peak at 284.8 eV as the reference. The diffuse reflection spectra (DRS) of the samples were recorded using a scan UV-vis spectrophotometer (Shimadzu UV-3600 plus) equipped with an integrating sphere assembly, and $BaSO_4$ was used as the reference.

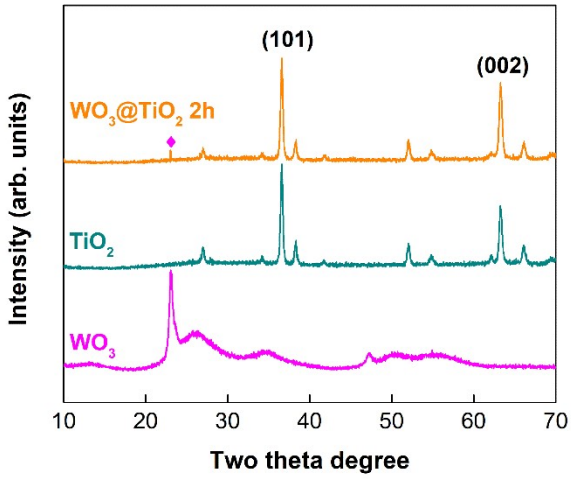

Fig. S1 XRD pattern of the as-prepared samples.

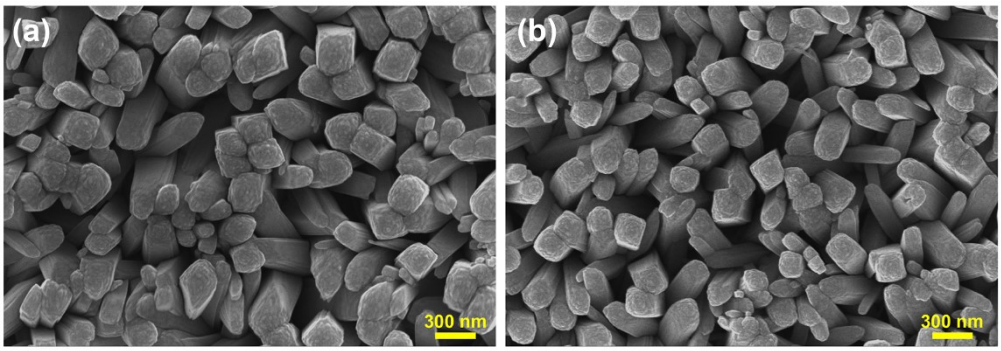

Fig. S2 FESEM images (top view) of the (a)TiO_2 nanowire arrays and (b) WO_3@TiO_2 2h samples.

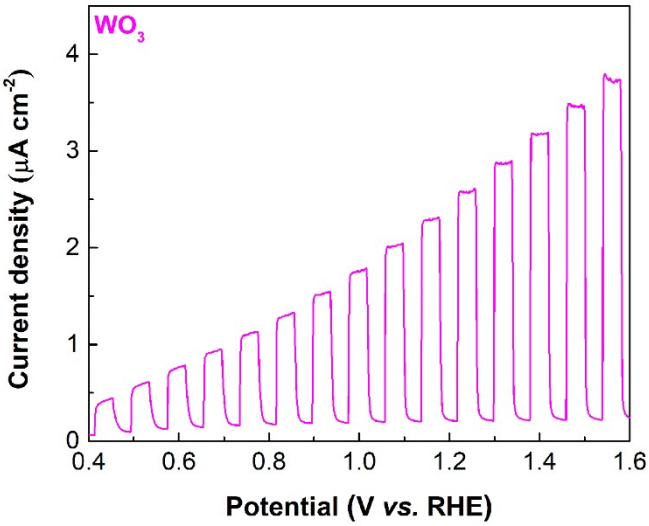

Fig. S3 Photocurrent density-potential curves of the WO_3 electrode.

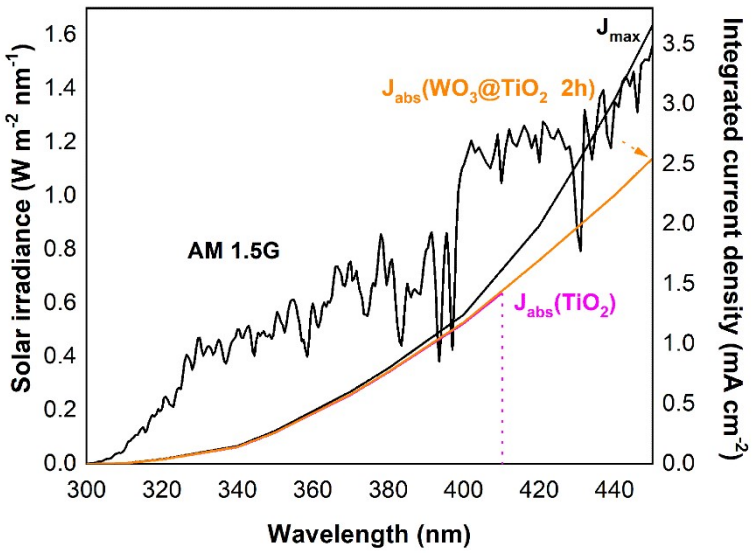

Figure S4. J_{max} and J_{abs} of the TiO_2 and WO_3@TiO_2 2h electrodes under AM 1.5G irradiation. J_{max} curve is calculated using a trapezoidal integration of AM 1.5G spectrum. The J_{abs} curve was obtained via multiply the AM 1.5G solar spectrum with absorption spectrum and then integrate.

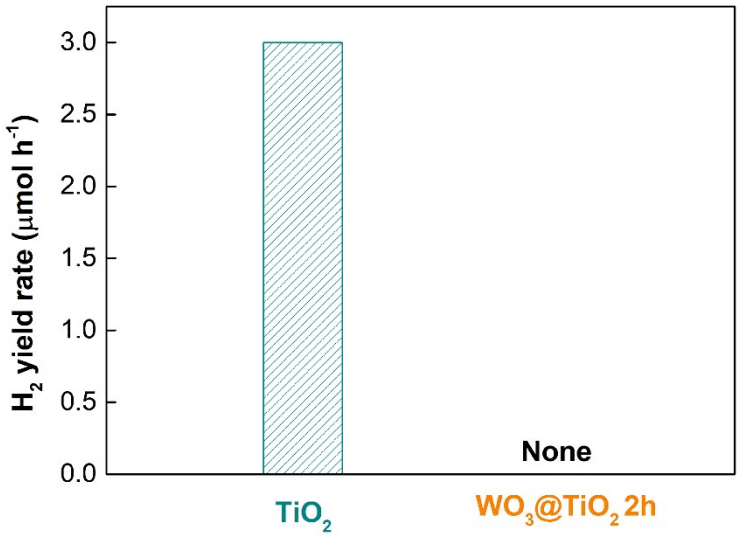

Fig.S5 Photocatalytic performance of different electrodes (methanol (10 vol.%) as sacrificial agent; 300W Xenon lamp; photodeposition of Pt (2 wt.%)).

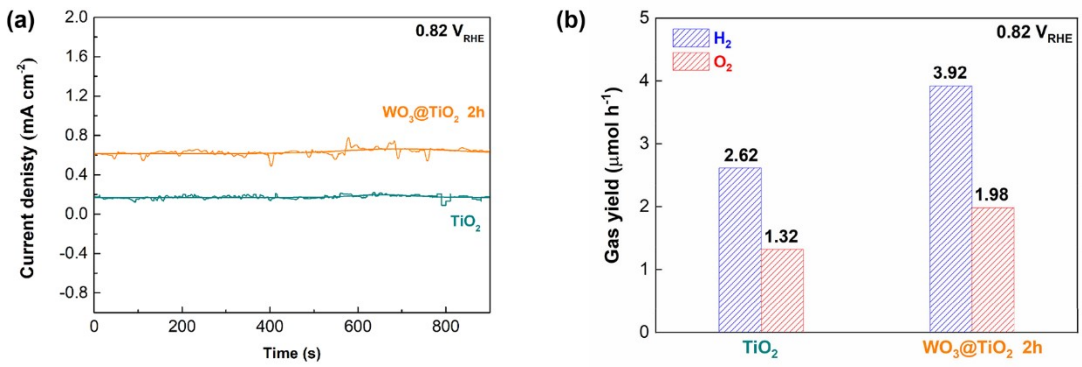

Fig. S6 (a) Steady-state photocurrent density at 0.2 V *vs.* Ag/AgCl (0.82 V *vs.* RHE) for the TiO_2 and WO_3@TiO_2 2h photoanodes; (b) Photoelectrocatalytic overall water splitting with the TiO_2 and WO_3@TiO_2 2h as photoanodes at 0.2 V *vs.* Ag/AgCl (0.82 V *vs.* RHE).

Table S1 Summary of PEC performance of WO_3-based and TiO_2-based photoanodes

Photoanode	Light	Photocurrent density at 1.23 V_{RHE} (mA cm^{-2})	H_2 yield rate (μmol h^{-1}) at 1.23 V_{RHE}	O_2 yield rate (μmol h^{-1}) at 1.23 V_{RHE}	Ref.
γ-graphyne/TiO_2	AM1.5 G (100 mW cm^{-2})	0.75	/	/	1
WO_3/TiO_2 nanoplates	AM1.5 G (100 mW cm^{-2})	0.25	/	/	2
TiO_2@g-CN nanorods arrays	AM1.5 G (100 mW cm^{-2})	0.91	/	/	3
WO_3@α-Fe_2O_3	AM1.5 G (100 mW cm^{-2})	1.66	/	/	4
WO_{3-x}@TiO_{2-x}	500 W Xe lamp (100 mW cm^{-2})	~3.2	56	27	5
TiO_2/$BiVO_4$/SnO_2	AM1.5 G (100 mW cm^{-2})	~2.3	/	/	6
WO_{3-x}/TiO_2	300 W Xe lamp (320 mW cm^{-2})	4.16	69.6 (1.2 V_{RHE})	~34.8 (1.2 V_{RHE})	7
BN ZnO/TiO_2	AM1.5 G (100 mW cm^{-2})	2.75	45.6	21.8	8
α-Fe_2O_3/Au/TiO_2	AM1.5 G (100 mW cm^{-2})	1.05	18.67	9.24	9
WO_3@TiO_2 2h	AM1.5 G (100 mW cm^{-2})	**~ 1.5**	**14.42**	**7.25**	**This work**

Reference

1. D. Qiu, C. He, Y. Lu, Q. Li, Y. Chen and X. Cui, *Dalton T.*, 2021, **50**, 15422-15432.
2. K. I. Liu and T. P. Perng, *ACS Appl. Energy Mater.*, 2020, **3**, 4238-4244.
3. L. Wang, R. Wang, L. Feng and Y. Liu, *J. Am. Ceram. Soc.*, 2020, **103**, 6272-6279.
4. Y. Li, L. Zhang, R. Liu, Z. Cao, X. Sun, X. Liu and J. Luo, *ChemCatChem*, 2016, **8**, 2765-2770.
5. K. Yuan, Q. Cao, H.-L. Lu, M. Zhong, X. Zheng, H.-Y. Chen, T. Wang, J.-J. Delaunay, W.

Luo and L. Zhang, *J. Mater. Chem. A*, 2017, **5**, 14697-14706.

6. S. W. Hwang, J. U. Kim, J. H. Baek, S. S. Kalanur, H. S. Jung, H. Seo and I. S. Cho, *J. Alloy. Compd.*, 2019, **785**, 1245-1252.
7. S. Lin, H. Ren, Z. Wu, L. Sun, X.-G. Zhang, Y.-M. Lin, K. H. Zhang, C. J. Lin, Z. Q. Tian and J. F. Li, *J. Energy Chem.*, 2021, **59**, 721-729.
8. T. Zhou, J. Wang, S. Chen, J. Bai, J. Li, Y. Zhang, L. Li, L. Xia, M. Rahim and Q. Xu, *Appl. Catal. B: Environ.*, 2020, 267, 118599.
9. Y. Fu, C. L. Dong, W. Zhou, Y. R. Lu, Y. C. Huang, Y. Liu, P. Guo, L. Zhao, W. C. Chou and S. Shen, *Appl. Catal. B: Environ.*, 2020, 260, 118206.